Original article

Short term evaluation of right ventricular function using speckle tracking echocardiography before and after trans-catheter device closure of atrial septal defects in children

Omar Raafat, Ahmed El-Nawawy, Aly Abdel Mohsen, Hani M. Adel
Department of pediatrics, Faculty of Medicine, Alexandria University, Alexandria, Egypt

Abstract. *Background:* Atrial septal defect (ASD) is a common congenital heart defect (CHD) in children. Evaluating right ventricular (RV) function is essential to understand the impact of ASD and its treatment. Speckle tracking echocardiography (STE) provides a reliable, non-invasive method for detailed RV function assessment. *Aims:* This study aimed to assess RV function in children with ASD before and after transcatheter device closure using STE. *Methods:* A case-control study was conducted in the catheterization lab at Smouha Children's Hospital, University of Alexandria, Egypt. It included 50 children under 18 years with ostium secundum ASD undergoing transcatheter device closure and 50 age-matched controls. Transthoracic echocardiography evaluated RV function through parameters such as RV fractional area change (FAC), myocardial performance index (MPI or Tei index), annular pulsed tissue Doppler imaging (TDI), and tricuspid annular plane systolic excursion (TAPSE). Right ventricular free wall strain (RVFW strain) was measured offline using 2D STE software (TomTec). *Results:* Significant improvement in RVFW strain was observed following ASD closure, with progressive enhancement at one- and three-months post-procedure. Parameters such as TAPSE, FAC, and RV MPI also showed improvement, indicating recovery of RV systolic function. *Conclusion:* ASD is associated with reduced RV contractility and myocardial deformation, primarily due to volume overload. Following transcatheter device closure, RV function improved significantly over time. STE is an effective tool for detecting global and regional myocardial dysfunction and monitoring functional recovery after ASD closure. (www.actabiomedica.it)

Key words: atrial septal defects, speckle tracking, strain, trans-catheter, echocardiography

Background

Atrial septal defect (ASD) is among the most common congenital heart defects (CHD) in children (1), often presenting as an isolated defect or in combination with other congenital cardiac abnormalities (2). Most isolated ASDs are asymptomatic during childhood and adolescence, with even large ASDs sometimes remaining undetected until adulthood (3). In rare cases, infants with large ASDs may present with symptoms such as heart failure, tachypnea, recurrent respiratory infections, or failure to thrive (4). The echocardiographic evaluation of right ventricular (RV) function employs various parameters. Visual inspection, or "eyeballing," is the simplest and most commonly used method. However, studies have demonstrated that relying solely on visual assessment is insufficient for an accurate evaluation of RV function, and its applicability in different clinical settings remains unclear (5,6). Current guidelines recommend supplementing visual assessment with at least one quantitative echocardiographic measure (7). Established parameters include tricuspid annular plane systolic excursion (TAPSE), tissue Doppler imaging (TDI), fractional area change

(FAC), myocardial performance index (MPI), and longitudinal strain assessed via speckle tracking echocardiography (STE) (7,8). Myocardial strain, defined as the percentage change in the myocardium's shape relative to its original form, offers valuable insights into RV function. Using STE, RV longitudinal strain (RVLS) can be quantified, specifically focusing on RV free-wall longitudinal strain (FWLS) and RV global longitudinal strain (GLS) from the apical RV-focused four-chamber view (9). Unlike left ventricular function, RV function is characterized by distinct mechanics, including greater free tricuspid annular motion toward the apex, higher longitudinal regional velocities, and reduced circumferential shortening velocities (7,10). Although techniques such as TDI have been extensively used to evaluate RV function post-ASD device closure, studies employing STE for this purpose remain limited (11,12). This study aims to address this gap by assessing the short-term effects of transcatheter device closure of ASDs on RV function in children using STE.

Methods

Study design and sample size

This prospective case-control study was conducted in the catheterization lab unit at Smouha Children's Hospital, University of Alexandria, Egypt. The study included 50 patients with ostium secundum atrial septal defects (ASDs) undergoing transcatheter device closure and 50 age- and sex-matched controls. The sample size was determined to achieve a statistical power of 80% at a 95% confidence level ($\alpha = 0.05$). The statistical analysis indicated that this sample size was sufficient to detect significant differences in the primary outcomes.

Patient selection

The study included 100 participants selected according to predefined inclusion and exclusion criteria. Ethical approval was obtained from the Alexandria University Ethical Committee (Serial Number: 0201787, IRB No: 00012098, FWA No: 00018699, Year: 2022). Informed consent was obtained from the parents or legal guardians of all participating children prior to the start of the study, in accordance with the principles of the Declaration of Helsinki and its later amendments in 2020.

Inclusion criteria

Children under 18 years of age with hemodynamically significant ostium secundum ASDs eligible for device closure. Presenting symptoms included decreased exercise tolerance, easy fatigability, palpitations, recurrent chest infections, failure to thrive, syncope, and right ventricular (RV) volume overload or dilatation. Adequate surrounding rim of ≥5 mm from the mitral valve, right upper pulmonary vein, coronary sinus, tricuspid valve, inferior vena cava, and superior vena cava was required for ASD device closure (13-15). Percutaneous closure was allowed in cases with deficient or absent aortic rim (<5 mm), provided the remaining rims were adequate.

Exclusion criteria

Children with other congenital heart defects, sinus venosus ASDs, primum ASDs, coronary sinus defects, or atrioventricular rim <5 mm, and patients with severe pulmonary hypertension.

Echocardiographic assessment

All participants underwent transthoracic echocardiography (TTE) performed by an experienced echocardiographer using the Philips EPIQ 7 C system with an X5-1 probe (Philips Medical Systems, Andover, MA, USA). Echocardiographic evaluations were conducted before, during, and after transcatheter ASD closure to assess RV function.

Conventional two-dimensional echocardiography (2D TTE)

ASD size, surrounding rims, and associated congenital heart anomalies were evaluated. RV and left ventricular (LV) diameters were measured in the apical four-chamber view. The RV/LV ratio was determined from the parasternal short-axis view at the papillary muscle level.

RV fractional area change (FAC)

FAC was calculated as (RVEDA–RVESA)/RVEDA(RVEDA - RVESA) / RVEDA (RVEDA–RVESA)/RVEDA, where RVEDA is the end-diastolic area and RVESA is the end-systolic area.

Tissue Doppler Imaging (TDI)

Annular pulsed TDI was performed to measure the myocardial performance index (MPI or Tei index).

Speckle tracking echocardiography (STE)

A frame rate of 80–100 frames per second was maintained. Three continuous cardiac cycles were recorded, and images with the clearest myocardial wall delineation were selected for analysis. The two-dimensional speckle tracking offline analysis software from TomTec was used to assess RV strain. Automated RV strain analysis tracked the endocardial borders, generating RV longitudinal strain curves for apical, mid, and basal free wall segments. The software provided average strain values, referred to as global longitudinal strain (GLS), to evaluate overall RV function (16).

Validation of speckle tracking analysis

The validity of the analysis was confirmed through visual inspection of the tracking quality and the software's automated outputs. RV longitudinal strain parameters, including RV free-wall longitudinal strain (FWLS) and GLS, were used to evaluate global and regional RV function. This revised methods section ensures clarity, coherence, and technical accuracy while maintaining readability and a professional tone.

Intervention phase

The atrial septal defect (ASD) closures were performed using a percutaneous transcatheter approach with devices such as the Amplatzer Septal Occluder, Occlutech Septal Occluder, or Lifetech Cera ASD Occluder. All procedures were conducted under general anesthesia with guidance from fluoroscopy and transthoracic echocardiography (TTE). In cases were suboptimal echo images were obtained, transesophageal echocardiography (TEE) was used to enhance visualization of the ASD rims and aid in device placement. The maximum ASD diameter was measured from various views during 2D TTE and 2D TEE. The device size was determined by adding 2–6 mm to the largest measured diameter. Post-procedure care was provided in the post-catheter intermediate care unit at Smouha Children's Hospital. Follow-up included: (a) Electrocardiogram (ECG) and chest X-rays (postero-anterior and lateral views) to confirm device positioning, (b) Echocardiographic evaluation one day post-procedure (17).

Prescription of oral acetyl salicylic acid 5 mg/kg/day for six months to prevent thromboembolic complications.

Statistical analysis

Data analysis was performed using IBM SPSS software (version 20.0; IBM Corp., Armonk, NY). Qualitative variables were presented as frequencies and percentages. Quantitative data were assessed for normality using the Shapiro-Wilk test and described using appropriate measures, including range (minimum and maximum), mean and standard deviation, median and interquartile range (IQR). A P value < 0.05 was considered statistically significant.

Results

As detailed in Table 1, the study population comprised 50 pediatric patients who underwent transcatheter ASD closure (46% male, 54% female) and 50 control subjects (60% male, 40% female). The ages of ASD patients ranged from 2 to 16 years (mean: 5.42 years, range: 3.0–7.0 years), while the ages of the control group spanned 3 to 13 years (median: 5.46 years, range: 3.67–7.0 years). The weight of ASD patients ranged from 10 to 45 kg (median: 18.5 kg, range: 14.0–26.0 kg), compared to the control group's weight of 10 to 35 kg (median: 19.5 kg, range: 16.0–22.0 kg).

Table 1. Comparison between the ASD cases group and control group according to demographic data and echocardiographic parameters. Data are presented as mean ± standard deviation (SD) or median (interquartile range, IQR) as appropriate**.**

Parameter	Cases (n=50)	Controls (n=50)	P-value
TAPSE (cm)	1.62 ± 0.24	1.94 ± 0.12	**< 0.001**
RV/LV Ratio	0.79 ± 0.18	0.44 ± 0.03	**< 0.001**
FAC (%)	25.24 ± 5.03	40.28 ± 1.90	**< 0.001**
RV MPI	0.54 ± 0.06	0.29 ± 0.02	**< 0.001**
RVFW Strain (%)	21.0 (18.20 – 24.30)	32.0 (29.50 – 33.0)	**< 0.001**
Apical Free Wall Strain (%)	17.78 ± 3.85	24.18 ± 2.04	**< 0.001**
Mid Free Wall Strain (%)	22.34 ± 5.36	30.23 ± 4.38	**< 0.001**
Basal Free Wall Strain (%)	26.07 ± 5.28	38.0 ± 4.51	**< 0.001**
RVGLS (%)	19.69 ± 4.13	28.76 ± 0.91	**< 0.001**

Abbreviations: TAPSE = Tricuspid Annular Peak Systolic Excursion; RVFW = Right Ventricular Free Wall; RVGLS = Right Ventricular Global Longitudinal Strain; Bold P-values indicate statistical significance.

Table 2. Distribution of the ASD cases according to device data and procedure characteristics.

Parameters	No. (%)
Device type	
Amplatzer	41 (82.0%)
Life tech	6 (12.0%)
Occlutech	3 (6.0%)
Device size	
Min. – Max.	10.0 – 38.0
Mean ± SD.	18.26 ± 6.88
Device/ASD size	
Min. – Max.	1.0 – 1.50
Mean ± SD.	1.16 ± 0.11
Device/weight	
Min. – Max.	0.33 – 2.10
Mean ± SD.	0.97 ± 0.38
Procedure time (min)	
Min. – Max.	24.0 – 38.0
Mean ± SD.	29.02 ± 3.25
Fluoroscopy time (min)	
Min. – Max.	4.0 – 8.60
Mean ± SD.	6.16 ± 1.11

Abbreviations: SD: Standard deviation.

Pre-closure comparisons between ASD patients and controls revealed significant differences in echocardiographic parameters. Tricuspid annular plane systolic excursion (TAPSE) was significantly lower in ASD patients than in controls (P: <0.001). The right ventricular to left ventricular (RV/LV) ratio was significantly higher in ASD patients (P: <0.001) indicating RV enlargement. Additionally, RV fractional area change (FAC) was markedly reduced in ASD patients compared to controls (P: <0.001). RV myocardial performance index (MPI) was significantly elevated in the ASD group (P: <0.001) reflecting impaired RV function. Similarly, strain parameters derived from speckle tracking echocardiography (STE), including RV free-wall longitudinal strain (RVFW strain), apical RVFW strain, mid RVFW strain, basal RVFW strain, and RV global longitudinal strain (RVGLS), were significantly lower in ASD patients compared to controls (P: <0.001). These findings underscore the adverse impact of ASD on RV function and highlight the utility of both conventional and advanced echocardiographic measures in assessing myocardial performance in this population. Table 2 shows type of ASD device and its size and its relation to patient weight with the mean device size: 18.26± 6.88, mean device size to ASD size ratio: 1.16± 0.11 and mean device size to patient weight ratio: 0.97 ±0.38.

As reported in Table 3, while there was a notable improvement in RVMPI following the closure of the ASD device, the ASD group displayed significantly higher levels three months post-closure in comparison to the control group (P: < 0.001). Furthermore, three months after closure, the ASD group exhibited considerably lower RVFW longitudinal strain, apical

Table 3. Comparison between ASD cases 3 months after device closure and control group regarding echocardiographic parameters. Data are presented as mean ± standard deviation (SD) or median (interquartile range, IQR) as appropriate.

Parameter	Cases (n = 50)	Controls (n = 50)	P-value
TAPSE (cm)			**< 0.001**
Min – Max	1.67 – 2.50	1.80 – 2.30	
Mean ± SD	2.05 ± 0.17	1.94 ± 0.12	
RV/LV Ratio			**< 0.001**
Min – Max	0.37 – 0.62	0.38 – 0.49	
Mean ± SD	0.48 ± 0.06	0.44 ± 0.03	
FAC (%)			**< 0.001**
Min – Max	35.0 – 58.0	37.0 – 43.0	
Mean ± SD	44.38 ± 5.77	40.28 ± 1.90	
RV MPI			**< 0.001**
Min – Max	0.29 – 0.50	0.25 – 0.32	
Mean ± SD	0.40 ± 0.05	0.29 ± 0.02	
RVFW Strain (%)			**< 0.001**
Min – Max	23.50 – 39.20	28.30 – 38.20	
Median (IQR)	28.6 (26.5 – 32.2)	32.0 (29.5 – 33.0)	
Apical Free Wall Strain (%)			**0.027**
Min – Max	15.60 – 30.40	20.80 – 29.20	
Mean ± SD	22.83 ± 3.70	24.18 ± 2.04	
Mid Free Wall Strain (%)			0.496
Min – Max	21.30 – 39.50	26.0 – 43.50	
Mean ± SD	29.60 ± 4.86	30.23 ± 4.38	
Basal Free Wall Strain (%)			0.140
Min – Max	24.70 – 47.10	31.0 – 48.0	
Mean ± SD	36.54 ± 5.26	38.0 ± 4.51	
RVGLS (%)			**< 0.001**
Min – Max	20.0 – 38.80	27.0 – 31.30	
Mean ± SD	26.85 ± 3.30	28.76 ± 0.91	

Abbreviations: TAPSE =Tricuspid annular peak systolic excursion; RV/LV ratio = right ventricle/left ventricle ratio; RVFW strain = right ventricular free wall strain; RVGLS = right ventricular Global longitudinal strain; Bolded P-values clearly mark statistical significance.

RVFW strain, and RVGLS when compared to the control group (P: < 0.001).

In a study comparing various timeframes before and after the closure of the ASD device regarding the dimensions of the right atrium's long and short axes, as shown in Table 4, there was a significant reduction in the long axis width of the right atrium from before the ASD device closure to day 1 following the procedure (P: < 0.001), one month post-closure (P: < 0.001), and three months post-closure (P: < 0.001). Additionally, the long axis diameter of the right atrium also experienced a significant decrease from pre-ASD device closure to day 1 after the procedure (P: < 0.001), one month later (p < 0.001), and three months after the closure (P: < 0.001). Table 4 presents a comparison of the various assessed time points before and after the ASD device closure regarding the long and short axis diameters of the RV. There was a marked reduction in the long axis diameter of the RV from the pre-ASD device closure measurement to day 1 following

Table 4. Comparison of right atrium (RA) and right ventricle (RV) axis diameters before and after ASD device closure.

Parameter	Pre (mean ± SD)	1 day (mean ± SD)	1 month (mean ± SD)	3 months (mean ± SD)	P-value
RA Long Axis Diameter (cm)	3.37 ± 0.34	3.17 ± 0.34	3.03 ± 0.37	2.89 ± 0.39	**< 0.001**
RA Short Axis Diameter (cm)	2.89 ± 0.31	2.69 ± 0.32	2.54 ± 0.31	2.40 ± 0.30	**< 0.001**
RV Long Axis Diameter (cm)	4.41 ± 0.47	4.22 ± 0.45	4.07 ± 0.43	3.96 ± 0.42	**< 0.001**
RV Short Axis Diameter (cm)	2.99 ± 0.29	2.80 ± 0.26	2.64 ± 0.26	2.52 ± 0.25	**< 0.001**

Table 5. Comparison of TAPSE, FAC and RVMPI before and after ASD device closure.

Parameter	Pre	1 day	1 month	3 months	P-value
TAPSE (cm)					
Min – Max	1.20-2.30	1.20 – 1.90	1.50 – 2.30	1.67 – 2.50	< 0.001
Mean ± SD	1.62 ± 0.24	1.48 ± 0.20	1.88 ± 0.20	2.05 ± 0.17	
P0	-	0.001	<0.001	<0.001	
Significance between periods					P1: < 0.001 P2:< 0.001 P3: < 0.001
FAC (%)					
Min – Max	17.0 – 35.0	21.0 – 42.0	24.0 – 49.0	35.0 – 58.0	< 0.001
Mean ± SD	25.24 ± 5.03	32.02 ± 4.83	38.64±5.15	44.38 ± 5.77	
P0	-	<0.001	<0.001	<0.001	
Significance between periods					P1: < 0.001 P2:< 0.001 P3: < 0.001
RVMPI					
Min – Max	0.42 – 0.69	0.46– 0.72	0.31 – 0.58	0.29 – 0.50	<0.001
Mean ± SD	0.54 ± 0.06	0.58 ± 0.06	0.47 ± 0.06	0.40 ± 0.05	
P0	-	<0.001	<0.001	<0.001	
Significance between periods					P1: < 0.001 P2: < 0.001 P3: < 0.001

Abbreviations: P0: Significance of comparison to pre-closure values; P1: Comparison between pre-closure and 1 day post-closure; P2: Comparison between pre-closure and 1 month post-closure; P3: Comparison between pre-closure and 3 months post-closure; TAPSE=Tricuspid annular peak systolic excursion; FAC= fractional area change; RV MPI= right ventricular myocardial performance index.

the closure (P: < 0.001), as well as at one month (P: < 0.001) and three months (P: < 0.001) after the ASD device closure. Additionally, the long axis diameter of the RV showed a significant decrease from pre-ASD device closure to day 1 post-closure (P: < 0.001), one month after the procedure (P: < 0.001), and three months post-closure (P: < 0.001).

All measured parameters (RA and RV long and short axis diameters) decreased significantly from pre-closure values to 1 day, 1 month, and 3 months post-closure. The reductions were statistically significant across all time points (P:< 0.001). The greatest reductions were observed at 3 months post-closure, indicating progressive improvement over time. Based on data recorded in Table 5, the comparison between the different studied periods before and after ASD device closure regarding TAPSE (n = 50) revealed that there was significantly higher TAPSE over time from

Table 6. Comparison of RV speckle tracking echocardiography parameters before and after ASD device closure.

Parameter	Before ASD closure (Mean ± SD)	3 months after closure (Mean ± SD)	Significance (P-value)
RV free-wall strain (%)	21.60 ± 4.18	29.53 ± 3.93	< 0.001
Apical free-wall strain (%)	17.78 ± 3.85	22.83 ± 3.70	< 0.001
Mid free-wall strain (%)	22.34 ± 5.36	29.60 ± 4.86	< 0.001
Basal free-wall strain (%)	26.07 ± 5.28	36.54 ± 5.26	< 0.001
RV GLS (%)	19.69 ± 4.13	26.85 ± 3.30	< 0.001

Abbreviations: RV GLS: right ventricular global longitudinal strain.

before ASD device closure to 24 hours after ASD device closure (P: <0.001) to one month after ASD device closure (P: <0.001) to 3 months after ASD device closure (P: < 0.001). Table 5 confirmed that there was significantly lower RV MPI over time from pre-ASD device closure to 1-month post-ASD device closure (P: <0.001) to 3 months after ASD device closure (P: <0.001). There was a significantly higher RV MPI 24 hours post-ASD device closure compared to pre-ASD device closure (P: <0.001) with the mean decrease from pre-device closure to 3 months' post-closure being 0.13 ± 0.06. As clarified in Table 5, there was significantly lower RV MPI over time from pre-ASD device closure to 1-month post ASD device closure (P: <0.001) to 3 months after ASD device closure (p<0.001). There was a significantly higher RV MPI Day 1 post ASD device closure compared to pre-ASD device closure (P: <0.001) with the mean decrease from pre device closure to 3 months' post closure is (0.13 ± 0.06).

Table 6 demonstrates significant changes in speckle tracking echocardiography (STE) parameters over time before and after ASD device closure (n = 50). RV strain parameters (free-wall, apical, mid, and basal) showed a transient decrease immediately after ASD device closure on day 1. However, significant recovery and progressive improvement were observed at 1 month and continued at 3 months post-closure. This suggests an initial impact on RV function, followed by robust recovery over time. RV strain parameters (free-wall, apical, mid, and basal) showed a transient decrease immediately after ASD device closure on day 1. However, significant recovery and progressive improvement were observed at 1 month and continued at 3 months post-closure. This suggests an initial impact on RV function, followed by robust recovery over time. RV strain parameters (free-wall, apical, mid, and basal) showed a transient decrease immediately after ASD device closure on day 1. However, significant recovery and progressive improvement were observed at 1 month and continued at 3 months post-closure. This suggests an initial impact on RV function, followed by robust recovery over time.

Figures 1, 2 and 3 illustrate the progressive changes in right ventricular (RV) global and segmental strain measured by 2D speckle tracking echocardiography before and after atrial septal defect (ASD) device closure.

Discussion

In this study, we observed a significant reduction in right atrial and ventricular dimensions starting 24 hours post-transcatheter ASD closure, with progressive improvements noted over three months. These findings are consistent with prior studies (18-20). Pascotto et al. (20) also documented reductions in RV dimensions following ASD device closure due to decreased RV overload and dilation. Veldtman et al. (21) observed RV dimensional improvement within one month, while Ozturk et al. (22) and Yilmazer et al. (23) similarly reported reductions in RV size post-closure. Improvements in TAPSE at one- and three-months post-closure align with the observations of Vaidya et al. (24), indicating enhanced RV contractility and systolic function. These findings underscore the restoration of RV function following ASD closure and its positive impact on RV performance. The reduced

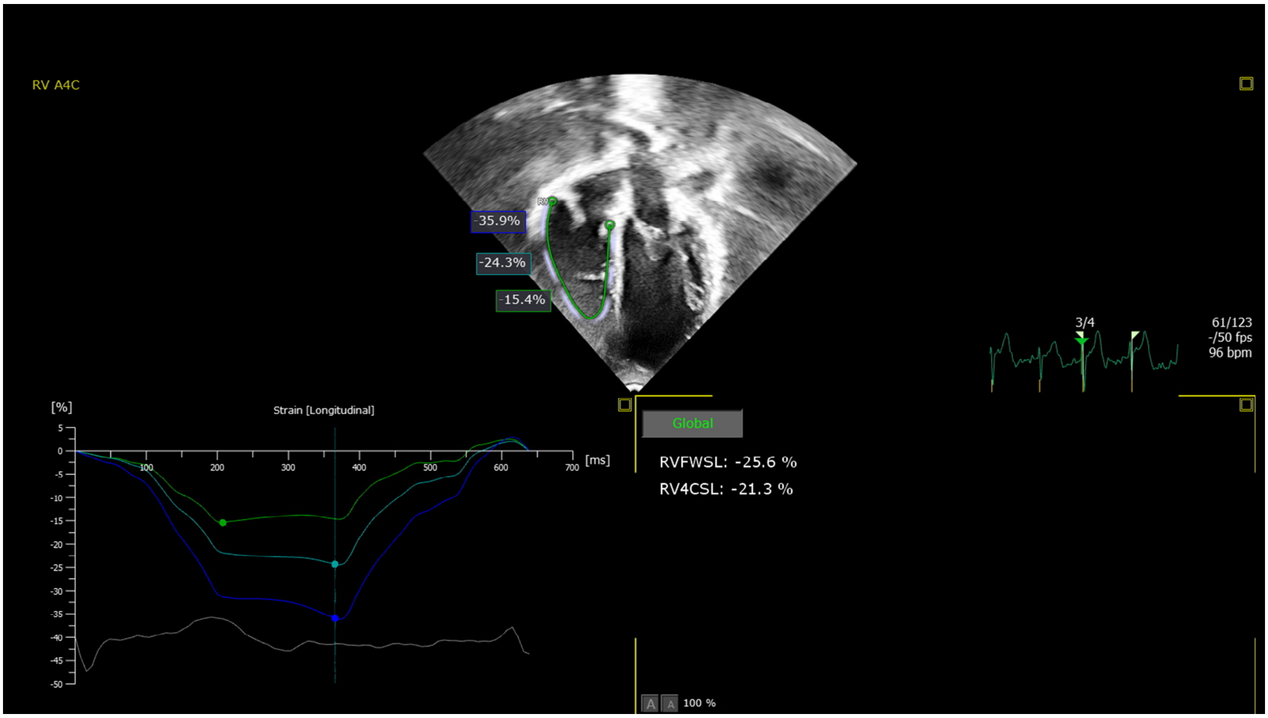

Figure 1. Shows RV global and segmental strain using 2D speckle tracking echocardiography before ASD device closure with right ventricular free wall longitudinal strain (RVFWSL)= 25.6%, right ventricular four chamber longitudinal strain (RV4CSL)=-21.3% , apical free wall longitudinal strain=-15.4%, mid-wall free wall longitudinal strain=-24.3%, basal free wall longitudinal strain=-35.9%.

TAPSE in ASD patients before closure compared to controls, as observed in our study, is consistent with Wang et al. (25), reflecting impaired RV systolic function due to volume overload. On the contrary, Balc et al. (26) reported unchanged TAPSE over follow-up, possibly due to residual RV impact in adults undergoing closure. Our findings of RV remodeling, including significant reductions in RV dimensions and MPI post-closure, align with results of Du et al. (19) and O'Byrne et al. (27). The improvements reflect favorable structural reverse remodeling and normalization of RV geometry due to reduced volume overload. Other studies similarly demonstrated maladaptive RV remodeling in pediatric ASD patients' pre-closure, followed by reverse remodeling post-closure (28-30). Elevated RV MPI in pre-closure ASD patients in our study aligns with Xu et al. (28), indicating impaired global RV function. Acute increases in MPI 24 hours post-closure may reflect transient changes in RV hemodynamics, while significant improvement at one and three months aligns with findings by Ding et al. (31) and Dhillon et al. (32).

RV Free-Wall Strain (RVFWLS) was significantly reduced in ASD patients before closure compared to controls, consistent with the other reports (33,34). Acute reductions in RVFWLS 24 hours post-closure, as observed in our study and others (28, 35), may result from sudden changes in RV hemodynamics. The gradual improvement in RVFWLS over three months reflects RV functional recovery, in line with Ghaderian et al. (36). Segmental RV Free-Wall Longitudinal Strain (FWLS) showed significantly impaired apical, mid, and basal strain in ASD patients pre-closure, with gradual improvement post-closure. These findings align with studies by Eroglu et al. (30) and Ko et al. (33). However, at three months, mid and basal FWLS normalized, while apical FWLS and global RV strain (RVGLS) remained impaired, consistent with Ghaderian et al. (36) and Ebaid et al. (37) studies. RVGLS, reduced in ASD patients pre-closure,

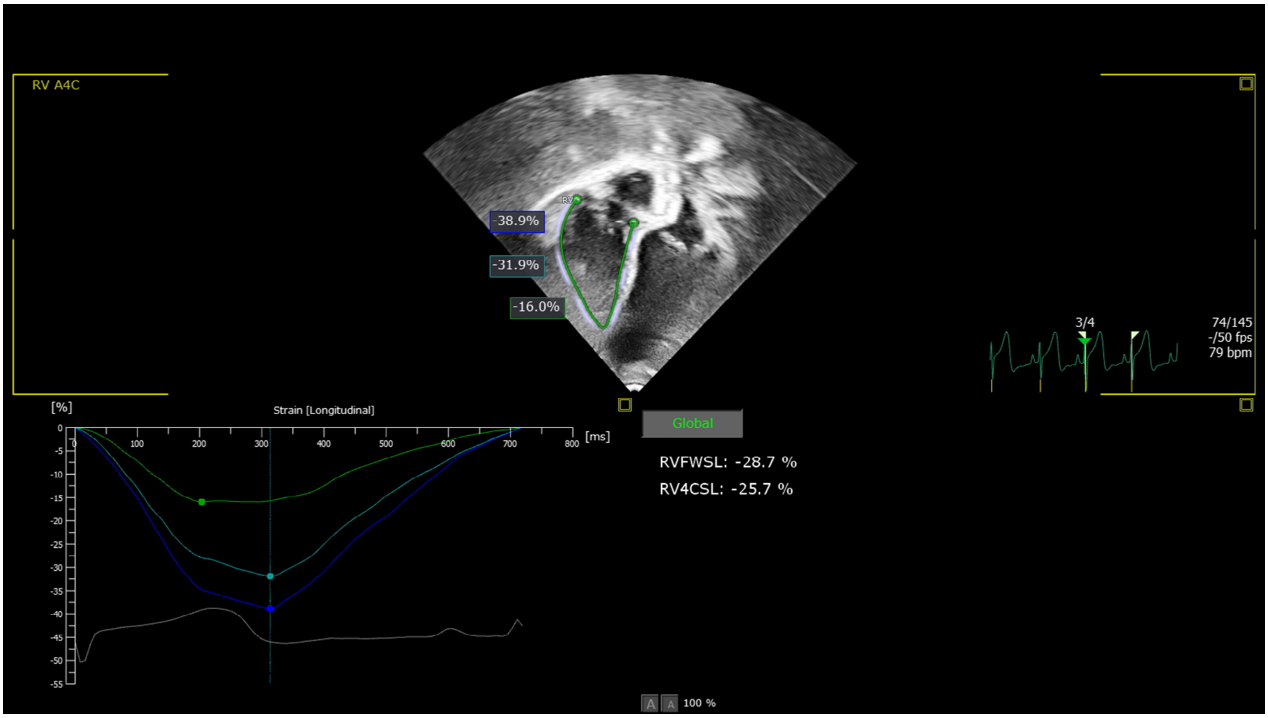

Figure 2. Shows improvement of RV global and segmental strain using 2D speckle tracking echocardiography 1-month after ASD device closure compared to before ASD closure with right ventricular free wall longitudinal strain (RVFWSL)=-28.7% , right ventricular four chamber longitudinal strain (RV4CSL)=-25.7%, apical free wall longitudinal strain=-16%, mid-wall free wall longitudinal strain=-31.9%, basal free wall longitudinal strain=-38.9%.

improved significantly post-closure over time. The transient decline in RVGLS 24 hours post-closure, as noted by Xu et al. (28) and Saedi et al. (38), may be due to acute hemodynamic changes. The subsequent recovery aligns with findings by Castaldi et al. (39) and Ozturk et al. (22). Despite improvements in RV strain parameters, RVFWLS and RVGLS did not fully normalize at three months post-closure, highlighting the need for longer follow-up. STE proves essential for detecting subtle myocardial dysfunction and assessing reverse remodeling, as demonstrated by Agha et al. (34). Substantially, our study adds the following findings:

1. A progressive improvement in RV global and segmental strain over time after closure.
2. Basal and mid-wall longitudinal strain of the RV returned to normal three months after ASD closure, whereas RV free-wall longitudinal strain (RVFWLS), apical RVFW strain, and global longitudinal strain (RVGLS) remained impaired at three months post-closure.
3. Continued assessment of RV STE parameters after ASD closure is recommended until normalization of all global and segmental RV functions.

Study limitations

This study focused on short-term follow-up of RV function after ASD device closure. Future studies with mid- and long-term follow-up are needed to evaluate the full extent of reverse remodeling and functional normalization.

Conclusion

Speckle tracking echocardiography (STE) effectively detects improvements in global and segmental

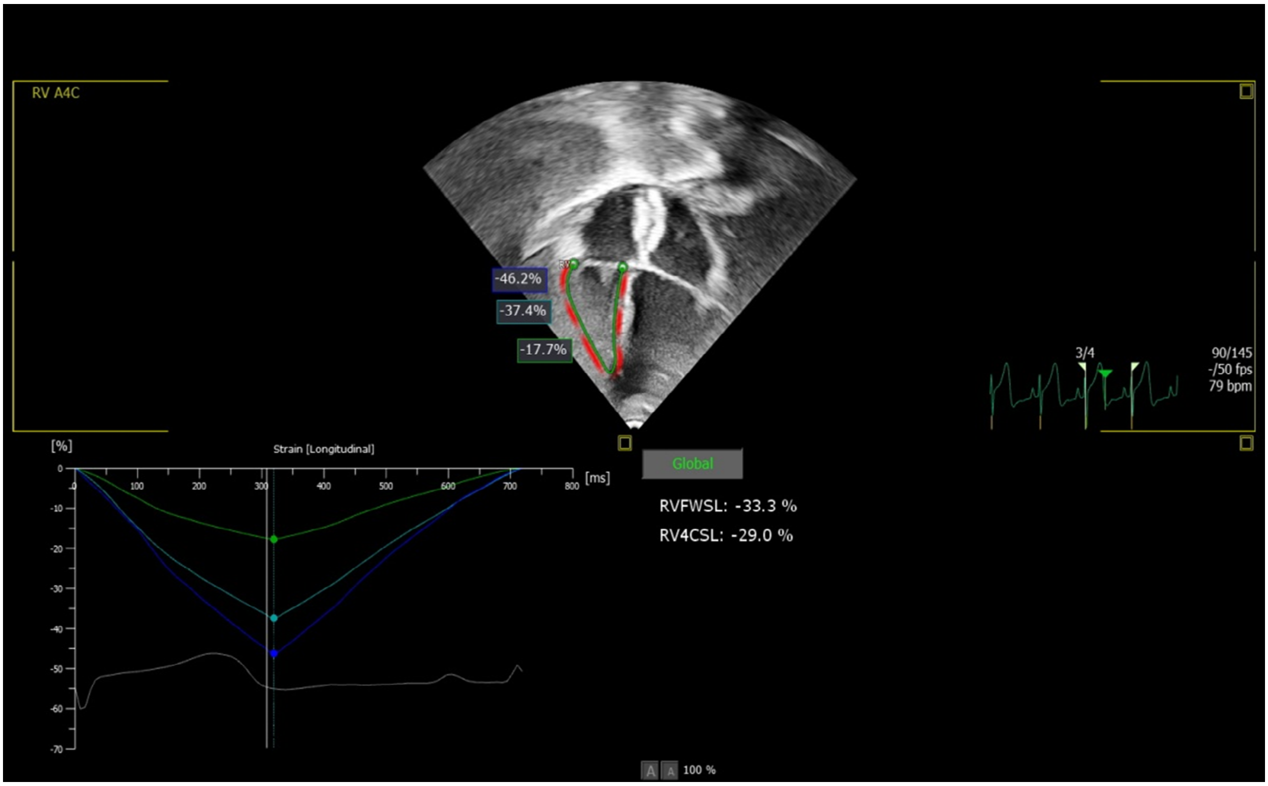

Figure 3. Shows improvement of RV global and segmental strain using 2D speckle tracking echocardiography 3-month after ASD device closure compare to previous time periods with right ventricular free wall longitudinal strain (RVFWSL)=-33.3%, right ventricular four chamber longitudinal strain (RV4CSL)=-29% , apical free wall longitudinal strain=-17.7%, mid-wall free wall longitudinal strain=-37.4%, basal free wall longitudinal strain=-46.2%

RV function following ASD closure. Serial STE evaluations over six months are recommended to monitor complete reverse remodeling and RV functional recovery.

Conflict of Interest: Each author declares that he or she has no commercial associations (e.g. consultancies, stock ownership, equity interest, patent/licensing arrangement etc.) that might pose a conflict of interest in connection with the submitted article.

Authors' Contributions: OR contributed to the study design, data collection, analysis, and drafting of the manuscript. AE supervised the study, critically reviewed the study design, and revised the manuscript for important intellectual content. AAM contributed to data interpretation and provided critical revisions to the manuscript. HMA ensured methodological accuracy, supervised the study, and contributed to the final preparation of the manuscript. All authors have read and approved the final version of the manuscript and agree to be accountable for all aspects of the work.

Acknowledgements: We thank all the participants in the study. We are also indebted to our colleagues for their help in facilitating this study.

Declaration of the Use of AI: None.

References

1. Jalal Z, Hascoet S, Baruteau AE, et al. Long-term complications after transcatheter atrial septal defect closure: a review of the medical literature. Can J Cardiol. 2016;32(11):1315.e11-e18. doi: 10.1016/j.cjca.2016.02.068.
2. Bhatt A, Landzberg M, Wu F. Atrial septal defect. Cardiology. 2010;3:1441-6.
3. Khairy P, Marelli AJ. Clinical use of electrocardiography in adults with congenital heart disease. Circulation. 2007;116(23):2734-46. doi: 10.1161/circulationaha.107.691568.
4. Andrews R, Tulloh R, Magee A, Anderson D. Atrial septal defect with failure to thrive in infancy: hidden pulmonary

vascular disease? Pediatr Cardiol. 2002;23(5):528-30. doi: 10.1007/pl00021008.

5. Zaidi A, Knight DS, Augustine DX, et al. Echocardiographic assessment of the right heart in adults: a practical guideline from the British Society of Echocardiography. Echo Res Pract. 2020;7(1):G19-G41. doi: 10.1530/erp-19-0051.
6. Ling LF, Obuchowski NA, Rodriguez L, Popovic Z, Kwon D, Marwick TH. Accuracy and interobserver concordance of echocardiographic assessment of right ventricular size and systolic function: a quality control exercise. J Am Soc Echocardiogr. 2012;25(7):709-13. doi: 10.1016/j.echo.2012.03.018.
7. Rudski LG, Lai WW, Afilalo J, et al. Guidelines for the echocardiographic assessment of the right heart in adults: a report from the American Society of Echocardiography endorsed by the European Association of Echocardiography and the Canadian Society of Echocardiography. J Am Soc Echocardiogr. 2010;23(7):685-788. doi: 10.1016/j.echo.2010.05.010.
8. Blanchard DG, Malouf PJ, Gurudevan SV, et al. Utility of right ventricular Tei index in the noninvasive evaluation of chronic thromboembolic pulmonary hypertension before and after pulmonary thromboendarterectomy. JACC Cardiovasc Imaging. 2009;2(2):143-9. doi: 10.1016/j.jcmg.2008.10.012.
9. Borges AC, Knebel F, Eddicks S, et al. Right ventricular function assessed by two-dimensional strain and tissue Doppler echocardiography in patients with pulmonary arterial hypertension and effect of vasodilator therapy. Am J Cardiol. 2006;98(4):530-4. doi: 10.1016/j.amjcard.2006.02.060.
10. Haber I, Metaxas DN, Geva T, Axel L. Three-dimensional systolic kinematics of the right ventricle. Am J Physiol Heart Circ Physiol. 2005;289(5):H1826-33. doi: 10.1152/ajpheart.00442.2005.
11. Schuuring MJ, Bolmers PP, Mulder BJ, et al. Right ventricular function declines after cardiac surgery in adult patients with congenital heart disease. Int J Cardiovasc Imaging. 2012;28(4):755-62. doi: 10.1007/s10554-011-9892-4.
12. Lakatos BK, Nabeshima Y, Tokodi M, Nagata Y, Tősér Z, Otani K, et al. Importance of nonlongitudinal motion components in right ventricular function: three-dimensional echocardiographic study in healthy volunteers. J Am Soc Echocardiogr. 2020;33(8):995-1005.e1. doi: 10.1016/j.echo.2020.04.002.
13. Godart F, Houeijeh A, Recher M, et al. Transcatheter closure of atrial septal defect with the Figulla ASD Occluder: a comparative study with the Amplatzer Septal Occluder. Arch Cardiovasc Dis. 2015;108(1):57-63. doi: 10.1016/j.acvd.2014.09.005.
14. Haas NA, Happel CM, Soetemann DB, et al. Optimal septum alignment of the Figulla Flex occluder to the atrial septum in patients with secundum atrial septal defects. EuroIntervention. 2016;11(10):1153-60. doi: 10.4244/eijy14m12_09.
15. Roymanee S, Promphan W, Tonklang N, Wongwaitaweewong K. Comparison of the Occlutech Figulla septal occluder and Amplatzer septal occluder for atrial septal defect device closure. Pediatr Cardiol. 2015;36(5):935-41. doi: 10.1007/s00246-015-1103-y.
16. Lee JH, Park JH. Strain analysis of the right ventricle using two-dimensional echocardiography. J Cardiovasc Imaging. 2018;26(3):111-24. doi: 10.4250/jcvi.2018.26.e11.
17. Bartakian S, El-Said HG, Printz B, Moore JW. Prospective randomized trial of transthoracic echocardiography versus transesophageal echocardiography for assessment and guidance of transcatheter closure of atrial septal defects in children. JACC Cardiovasc Interv. 2013;6(9):974-80. doi: 10.1016/j.jcin.2013.05.007.
18. Kort HW, Balzer DT, Johnson MC. Resolution of right heart enlargement after closure of secundum atrial septal defect with transcatheter technique. J Am Coll Cardiol. 2001;38(5):1528-32. doi: 10.1016/s0735-1097(01)01547-9.
19. Du ZD, Cao QL, Koenig P, Heitschmidt M, Hijazi ZM. Speed of normalization of right ventricular volume overload after transcatheter closure of atrial septal defect in children and adults. Am J Cardiol. 2001;88(12):1450-3, a9. doi: 10.1016/s0002-9149(01)02135-x.
20. Pascotto M, Santoro G, Caso P, et al. Global and regional left ventricular function in patients undergoing transcatheter closure of secundum atrial septal defect. Am J Cardiol. 2005;96(3):439-42. doi: 10.1016/j.amjcard.2005.03.096.
21. Veldtman GR, Razack V, Siu S, et al. Right ventricular form and function after percutaneous atrial septal defect device closure. J Am Coll Cardiol. 2001;37(8):2108-13. doi: 10.1016/s0735-1097(01)01305-5.
22. Ozturk O, Ozturk U, Zilkif Karahan M. Assessment of right ventricle function with speckle tracking echocardiography after the percutaneous closure of atrial septal defect. Acta Cardiol Sin. 2017;33(5):523-9. doi: 10.6515/acs20170106a.
23. Yılmazer MM, Güven B, Vupa-Çilengiroğlu Ö, et al. Improvement in cardiac structure and functions early after transcatheter closure of secundum atrial septal defect in children and adolescents. Turk J Pediatr. 2013;55(4):401-10.
24. Vaidya K, Khandkar C, Celermajer D. Current management aspects in adult congenital heart disease: non-surgical closure of patent foramen ovale. Cardiovasc Diagn Ther. 2018;8(6):739-53. doi: 10.21037/cdt.2018.09.09.
25. Wang JK, Tsai SK, Wu MH, Lin MT, Lue HC. Short- and intermediate-term results of transcatheter closure of atrial septal defect with the Amplatzer septal occluder. Am Heart J. 2004;148(3):511-7. doi: 10.1016/j.ahj.2004.01.030.
26. Balcı KG, Balcı MM, Aksoy MM, et al. Remodeling process in right and left ventricle after percutaneous atrial septal defect closure in adult patients. Turk Kardiyol Dern Ars. 2015;43(3):250-8. doi: 10.5543/tkda.2015.57106.
27. O'Byrne ML, Glatz AC, Gillespie MJ. Transcatheter device closure of atrial septal defects: more to think about than just closing the hole. Curr Opin Cardiol. 2018;33(1):108-16. doi: 10.1097/hco.0000000000000476.
28. Xu Q, Sun L, Zhou W, et al. Evaluation of right ventricular myocardial strains by speckle tracking echocardiography after percutaneous device closure of atrial septal defects in

children. Echocardiography. 2018;35(8):1183-8. doi: 10.1111/echo.14006.
29. Alkhateeb A, Roushdy A, Hasan-Ali H, Kishk YT, Hassan AKM. The changes in biventricular remodeling and function after atrial septal defect device closure and its relation to age of closure. Egypt Heart J. 2020;72(1):85. doi: 10.1186/s43044-020-00120-x.
30. Eroglu E, Cakal SD, Cakal B, et al. Time course of right ventricular remodeling after percutaneous atrial septal defect closure: assessment of regional deformation properties with two-dimensional strain and strain rate imaging. Echocardiography. 2013;30(3):324-30. doi: 10.1111/echo.12053.
31. Ding J, Ma G, Wang C, et al. Acute effect of transcatheter closure on right ventricular function in patients with atrial septal defect assessed by tissue Doppler imaging. Acta Cardiol. 2009;64(3):303-9. doi: 10.2143/ac.64.3.2038014.
32. Dhillon R, Josen M, Henein M, Redington A. Transcatheter closure of atrial septal defect preserves right ventricular function. Heart. 2002;87(5):461-5. doi: 10.1136/heart.87.5.461.
33. Ko HK, Yu JJ, Cho EK, et al. Segmental analysis of right ventricular longitudinal deformation in children before and after percutaneous closure of atrial septal defect. J Cardiovasc Ultrasound. 2014;22(4):182-8. doi: 10.4250/jcu.2014.22.4.182.
34. Agha HM, Mohammed IS, Hassan HA, Abu Seif HS, Abu Farag IM. Left and right ventricular speckle tracking study before and after percutaneous atrial septal defect closure in children. J Saudi Heart Assoc. 2020;32(1):71-8. doi: 10.37616/2212-5043.1012.
35. Kong D, Cheng L, Dong L, et al. Three-dimensional echocardiography in the evaluation of right ventricular global and regional systolic function in patients with atrial septal defect before and after percutaneous closure. Echocardiography. 2016;33(4):596-605. doi: 10.1111/echo.13134.
36. Ghaderian M, Dehghan B, Reza Sabri M, Ahmadi A, Sadeghi-Lotfabadi A. Evaluation of cardiac function in children after percutaneous closure of atrial septal defect using speckle tracking echocardiography. ARYA Atheroscler. 2020;16(6):290-4. doi: 10.22122/arya.v16i6.2128.
37. Ebaid HH, El Rabat KEED, Al-Emam AM, Mohamed MHA. Role of speckle tracking echocardiography in assessing right ventricle function after percutaneous closure of atrial septal defect. Cardiometry. 2024;31:110-8. doi: 10.18137/cardiometry.2024.31.110118.
38. Saedi T, Firouzi A, Saedi S. Cardiac remodeling after atrial septal defects device closure. Echocardiography. 2022;39(8):1089-94. doi: 10.1111/echo.15421.
39. Castaldi B, Santoro G, Di Candia A, et al. Impact of Gore Cardioform atrial septal defect occluder on atrial and ventricular electromechanics in a pediatric population. Am J Cardiol. 2024;211:259-67. doi: 10.1016/j.amjcard.2023.11.033.

Correspondence:

Received: 1 December 2024
Accepted: 7 January 2025

Omar Raafat, MD
Assistant Lecturer of Pediatrics, Faculty of Medicine, Alexandria University, Alexandria, Egypt
ORCID ID: 0000-0002-3056-4398
E-mail: o_riad16@alexmed.edu.eg